Discrimination of optical sources by use of adaptive blind source separation theory

Ivica Kopriva and Antun Peršin

Optical systems based on rotating reticles were invented to determine the polar coordinates of a primarily IR optical source. Such systems fail when several optical sources are present in their field of view simultaneously. It is demonstrated experimentally that this drawback can be overcome by the application of a blind-signal-separation algorithm on the output signals of a modified optical system. The separation of the modified optical system responses into independent components yields modulating functions that carry information concerning the polar coordinates of the corresponding single optical sources.

OCIS codes: 000.5490, 070.6110, 230.6120, 230.6080.

1. Introduction

An optical system that uses a rotating reticle is investigated. It is used to detect and determine the position of an object from which some form of primarily IR energy is emitted (see Fig. 1 where BP stands for bandpass filter).[1,2] For convenience, the optical system shown in Fig. 1 is called the optical tracker in this paper. A rotating reticle, also called a modulation disk, modulates the incidental optical flux $\Phi(\lambda, t)$ and is located in the focal plane of an optical imaging system. Depending on the shape of the clear and the opaque segments, the optical flux after the modulation disk (i.e., on the output of the photodetector) is modulated in the appropriate way. Frequency modulation (FM) is used most often, although it has been shown that FM is not far superior to amplitude modulation.[3] It has been pointed out that such optical trackers fail when several sources are present in their field of view simultaneously.[4] The objective of this paper is to show that this serious limitation of optical trackers can be overcome by the combined use of the theory of blind source separation (BSS) and an appropriate modification in the optical tracker design. BSS is an existing technique applied here, we believe for the first time, to reticle trackers.

In Section 2 we derive the qualitative mathematical model of the optical tracker output signal based on Fig. 1 and also of the output signals of the modified optical tracker (see Fig. 5). It is shown that the output signals are the convolved combinations of certain time-varying impulse responses and reticle-modulating functions. In Section 3, the foundations of BSS theory are discussed. It is shown that the modulating signals, which carry information about the polar coordinates of the optical sources, can be recovered on the basis of the observed signals, assuming only the convolutive model of the output signals. In Section 4 an adaptive BSS algorithm is described in detail while in Section 5 experimental results are presented. The statistical-independence assumption is experimentally verified in Section 6. Conclusions are in Section 7.

2. Derivation of the Signal Model

A fan-bladed pattern with clear and opaque segments, such as that shown in Fig. 2, is used to generate frequency-modulated flux. The deviation of the FM signal is directly proportional to the module of the polar coordinates (r, φ) of the optical source projection on the reticle area (Fig. 3), while the phase of the FM signal is equivalent to the polar coordinate phase. Based on Fig. 3, angle Ψ is given by

$$\Psi = \arctan \frac{r \sin \varphi + r_0 \sin \Omega_M t}{r \cos \varphi + r_0 \cos \Omega_M t} = \arctan \frac{\Delta \sin \varphi + \sin \Omega_M t}{\Delta \cos \varphi + \cos \Omega_M t}, \quad (1)$$

I. Kopriva is with Research and Development, Institute of Defense Studies, Bijenička 46, 10000 Zagreb, Croatia. A. Persin is with the Department of Laser Research and Development, Institute "Ruđer Bošković," Bijenička 54, 10000 Zagreb, Croatia.

Received 4 August 1998; revised manuscript received 2 November 1998.

0003-6935/99/071115-12$15.00/0

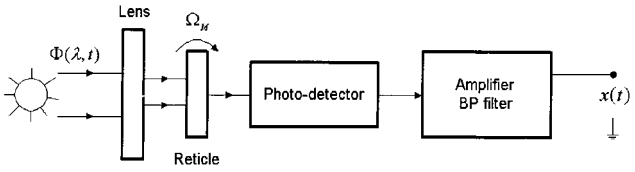

Fig. 1. Optical tracker. BP, bandpass.

where $\Delta = r/r_0$, which is the relative distance between the center of the circle with radius r_0 and the center of the reticle. The speed of the rotation of the optical source projection around the center of the reticle is given by

$$\omega(t) = \frac{d\Psi}{dt} = \frac{\Omega_M(1 + \Delta \cos \Omega_M t \cos \varphi + \Delta \, sin \, \Omega_M t \sin \varphi)}{1 + \Delta^2 + 2\Delta(\cos \Omega_M t \cos \varphi + sin \, \Omega_M t \sin \varphi)}. \quad (2)$$

When we multiply the numerator and the denominator of Eq. (2) by $1 - \Delta \cos \Omega_M t \cos \varphi - \Delta \sin \Omega_M t \sin \varphi$ and assume that $\Delta \ll 1$ allows for deleting all terms associated with the second and the third power of Δ, Eq. (2) becomes

$$\omega(t) = \Omega_M \frac{1 - \Delta^2(\cos \Omega_M t \cos \varphi + sin \, \Omega_M t \sin \varphi)^2}{1 + \Delta(\cos \Omega_M t \cos \varphi + sin \, \Omega_M t \sin \varphi)}. \quad (3)$$

When we apply the addition formula for the cosine of the angle difference and the rule for the difference of squares, Eq. (3) becomes

$$\omega(t) = \Omega_M[1 - \Delta \cos(\Omega_M t - \varphi)]. \quad (4)$$

For the reticle shown in Fig. 2 with n pairs of clear and opaque segments the instantaneous frequency of the source radiating flux after the reticle is given by

$$\hat{\omega}(t) = \omega_0 - \Delta\omega_m \cos(\Omega_M t - \varphi), \quad (5)$$

where

$$\omega_0 = n\Omega_M, \qquad \Delta\omega_m = \Delta n \Omega_M. \quad (6)$$

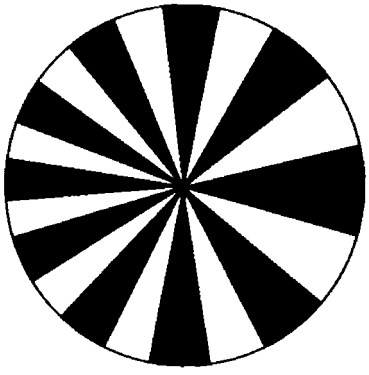

Fig. 2. Modulating disk with fan-bladed pattern.

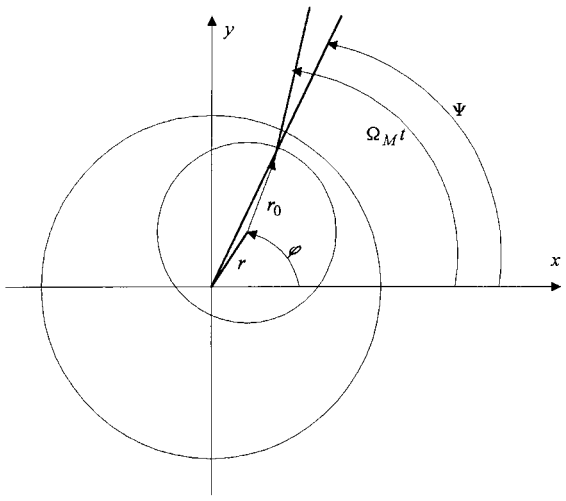

Fig. 3. Reticle coordinate system.

This situation is illustrated in Fig. 4. The time function with the instantaneous frequency that is based on Eq. (5) has the form

$$s(r, \varphi, t) = \cos[\omega_0 t - \beta \sin(\Omega_M t - \varphi)], \quad (7)$$

which is the canonical representation of an FM signal.[5] This waveform is actually the fundamental term of the photodetector response to the incident optical flux, which is illustrated in Fig. 4. The spectral terms around frequencies $2\omega_0$, $3\omega_0$, . . . exist, but the bandpass filter (see Fig. 1) removes these terms.[1,4] Consequently the incidental optical flux at the detector area can be described approximately as

$$\hat{\Phi}(\lambda, t) = \Phi(\lambda, t) \times s(r, \varphi, t). \quad (8)$$

The fundamental frequency of the reticle, $f_0 = nf_M$, is frequency modulated. The deviation of the FM sig-

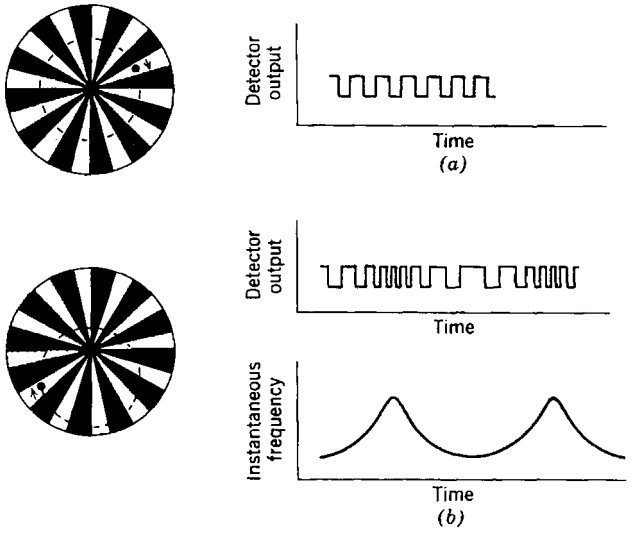

Fig. 4. Frequency-modulated signal generation principle (taken from Ref. 1).

nal, [Eq. (7)], i.e., the magnitude of the modulation, is given by

$$\beta = \frac{\Delta f_0}{f_M} = \frac{\Delta n f_M}{f_M} = \Delta n = n\,\frac{r}{r_0} = k \times r, \tag{9}$$

where n and r_0 are design constants. The deviation β is proportional to the radial distance of the image from the axis of rotation. An external phase reference must be provided to extract the phase information. By using elementary semiconductor theory,[6] we can show that the current response of the p-i-n photodiode to the incidental optical flux [Eq. (8)] is

$$i(\lambda) = A\,\frac{ch}{\lambda}\,\hat{\Phi}(\lambda, t)R(\lambda), \tag{10}$$

where A is the detector sensing area, c is the speed of light, h is Planck's constant, $R(\lambda)$ is the photodiode spectral responsivity, and λ is the wavelength. We obtain the total photocurrent by integrating Eq. (10) over the detector sensitivity range:

$$i(t) = Ahc \int_\lambda \frac{R(\lambda)\Phi(\lambda, t)}{\lambda}\,\mathrm{d}\lambda s(r, \varphi, t), \tag{11}$$

where $\hat{\Phi}(\lambda, t)$ is defined by Eq. (8). The amplifier output signal $x(t)$ (see Fig. 1) is obtained by the convolution of the impulse response $g(t)$ of the amplifier-bandpass filter and the input current of the form [Eq. (11)]:

$$x(t) = g(t) * i(t) = \int_0^t g(\tau)i(t - \tau)\mathrm{d}\tau. \tag{12}$$

Inserting Eq. (11) into Eq. (12), we obtain

$$x(t) = Ahc \int_0^t g(\tau) \int_\lambda \frac{R(\lambda)\Phi(\lambda, t - \tau)}{\lambda}\,\mathrm{d}\lambda s(r, \varphi, t - \tau)\mathrm{d}\tau. \tag{13}$$

Assuming that the photon flux $\Phi(\lambda, t)$ is a slowly varying function relative to $s(r, \varphi, t)$, we can replace the argument $t - \tau$ in Eq. (13) with τ and obtain

$$x(t) = Ahc \int_0^t \left[g(\tau) \int_\lambda \frac{R(\lambda)\Phi(\lambda, \tau)}{\lambda}\,\mathrm{d}\lambda \right] s(r, \varphi, t - \tau)\mathrm{d}\tau, \tag{14}$$

that is,

$$x(t) = \hat{g}(t) * s(r, \varphi, t), \tag{15}$$

where

$$\hat{g}(t) = g(t)Ahc \int_\lambda \frac{R(\lambda)\Phi(\lambda, t)}{\lambda}\,\mathrm{d}\lambda. \tag{16}$$

When two optical sources are present simultaneously in the optical tracker's field of view the photon flux after the reticle is of the form

$$\hat{\Phi}(\lambda, t) = \Phi_1(\lambda, t)s_1(r, \varphi, t) + \Phi_2(\lambda, t)s_2(r, \varphi, t), \tag{17}$$

where

$$s_1(r, \varphi, t) = s(r_1, \varphi_1, t), \qquad s_2(r, \varphi, t) = s(r_2, \varphi_2, t), \tag{18}$$

assuming that source S_1 is located at (r_1, φ_1) and source S_2 at (r_2, φ_2). Applying the same reasoning as above, for the optical tracker output signal we obtain

$$x(t) = g_1(t) * s_1(r, \varphi, t) + g_2(t) * s_2(r, \varphi, t), \tag{19}$$

where

$$g_1(t) = Ahcg(t) \int_\lambda \frac{R(\lambda)\Phi_1(\lambda, t)}{\lambda}\,\mathrm{d}\lambda,$$

$$g_2(t) = Ahcg(t) \int_\lambda \frac{R(\lambda)\Phi_2(\lambda, t)}{\lambda}\,\mathrm{d}\lambda. \tag{20}$$

Equation (19) shows that, when photodetector linearity is assumed, the optical tracker output signal is the convolved combination of the modulating functions (that carry information about the polar coordinates of the correspondent optical source) and the time-varying impulse responses of the form of Eq. (20). It has been shown analytically[4] that an optical tracker in such a case follows the centroid with the coordinates that are functions of the effective brightness of the two sources. In the case of two collinear sources located at points $(r_1, 0)$ and $(r_2, 0)$ with equal brightness, the optical tracker will see the coordinates $(e, 0)$ where

$$e = \frac{1}{2}\,(\beta_1 + \beta_2), \tag{21}$$

and β_1 and β_2 are the modulation magnitudes of the modulating signals $s_1(r, \varphi, t)$ and $s_2(r, \varphi, t)$ and are directly proportional to coordinates r_1 and r_2. The point of this discussion is that the optical tracker fails to determine the accurate coordinates of either of the two sources. The design of the optical tracker is modified to resolve this drawback (see Fig. 5). At this point, the reasons for performing such modification are not obvious. Note here that BSS theory (which will be used to solve the drawback mentioned) requires two observed signals for the source signals to be recovered. This theory is discussed in more detail in Section 3. The current response of two photodetectors on the incidental optical flux based on Fig. 5 is

$$i_1(t) = i_{11}(t)s_1(r, \varphi, t) + i_{12}(t)s_2(r, \varphi, t),$$

$$i_2(t) = i_{21}(t)s_1(r, \varphi, t) + i_{22}(t)s_2(r, \varphi, t), \tag{22}$$

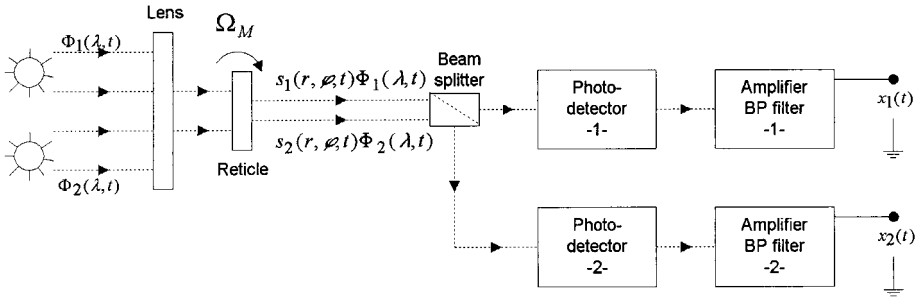

Fig. 5. Modified optical tracker.

where

$$i_{11}(t) = A_1 hc \int_\lambda \frac{\tau(\lambda) R_1(\lambda) \Phi_1(\lambda, t)}{\lambda} \, d\lambda,$$

$$i_{12}(t) = A_1 hc \int_\lambda \frac{\tau(\lambda) R_1(\lambda) \Phi_2(\lambda, t)}{\lambda} \, d\lambda,$$

$$i_{21}(t) = A_2 hc \int_\lambda \frac{\rho(\lambda) R_2(\lambda) \Phi_1(\lambda, t)}{\lambda} \, d\lambda,$$

$$i_{22}(t) = A_2 hc \int_\lambda \frac{\rho(\lambda) R_2(\lambda) \Phi_2(\lambda, t)}{\lambda} \, d\lambda.$$

Here $\rho(\lambda)$ is the beam-splitter reflection coefficient and $\tau(\lambda)$ is the beam-splitter transmission coefficient. The reticle-modulating functions $s_1(r, \varphi, t)$ and $s_2(r, \varphi, t)$ are defined by Eqs. (18). Output signals $x_1(t)$ and $x_2(t)$ are obtained by the convolution of photocurrents $i_1(t)$ and $i_2(t)$ with impulse responses $g_1(t)$ and $g_2(t)$, respectively:

$$x_1(t) = g_1(t) * i_1(t), \qquad x_2(t) = g_2(t) * i_2(t). \quad (23)$$

Assuming that photon fluxes $\Phi_1(\lambda, t)$ and $\Phi_2(\lambda, t)$ are a slowly varying function relative to modulating functions $s_1(r, \varphi, t)$ and $s_2(r, \varphi, t)$, the output signals are

$$x_1(t) = g_{11}(t) * s_1(r, \varphi, t) + g_{12}(t) * s_2(r, \varphi, t),$$
$$x_2(t) = g_{21}(t) * s_1(r, \varphi, t) + g_{22}(t) * s_2(r, \varphi, t), \quad (24)$$

where the * operator indicates a temporal convolution and the impulse responses $g_{11}(t)$, $g_{12}(t)$, $g_{21}(t)$, and $g_{22}(t)$ are

$$g_{11}(t) = A_1 hc g_1(t) \int_\lambda \frac{\tau(\lambda) R_1(\lambda) \Phi_1(\lambda, t)}{\lambda} \, d\lambda,$$

$$g_{12}(t) = A_1 hc g_1(t) \int_\lambda \frac{\tau(\lambda) R_1(\lambda) \Phi_2(\lambda, t)}{\lambda} \, d\lambda,$$

$$g_{21}(t) = A_2 hc g_2(t) \int_\lambda \frac{\rho(\lambda) R_2(\lambda) \Phi_1(\lambda, t)}{\lambda} \, d\lambda,$$

$$g_{22}(t) = A_2 hc g_2(t) \int_\lambda \frac{\rho(\lambda) R_2(\lambda) \Phi_2(\lambda, t)}{\lambda} \, d\lambda. \quad (25)$$

Equations (24) and (25) represent the mathematical model of the modified optical tracker output signals. It can be seen that the observed signals are the convolutive combination of the time-varying impulse responses given by Eqs. (25) and the reticle-modulating functions $s_1(r, \varphi, t)$ and $s_2(r, \varphi, t)$ that carry information about the polar coordinates of the projection of the optical sources on the reticle. The convolutive signal model described by Eqs. (24) is illustrated in Fig. 6 where $G_{11}(z, k)$, $G_{12}(z, k)$, $G_{21}(z, k)$, and $G_{22}(z, k)$ are Z transforms of the corresponding impulse responses given by Eqs. (25) and k is the discrete time index that implies that the impulse responses are nonstationary. By using BSS theory it is possible to recover source signals $s_1(r, \varphi, t)$ and $s_2(r, \varphi, t)$ on the basis of observed signals $x_1(t)$ and $x_2(t)$ only. The time-varying transfer functions $G_{11}(z, k)$, $G_{12}(z, k)$, $G_{21}(z, k)$, and $G_{22}(z, k)$ are assumed to be unknown. In the case of three or more sources the signal model generalization [Eqs. (24)] and the optical tracker modification shown in Fig. 5 are straightforward. For discrimination between three sources, two beam splitters and three photodetectors are necessary.

3. Interpretation of Theory Requirements for Blind Source Separation

BSS is a fundamental problem in signal processing. The problem is described in terms of a number of source signals coming from different sources and a number of receivers.[7] Each receiver (antenna, microphone, photodiode, etc.) receives a linear combination of these source signals. Neither the structure of the linear combination nor the source signals are known to the receivers. In this environment the identification of the linear combinations is called the

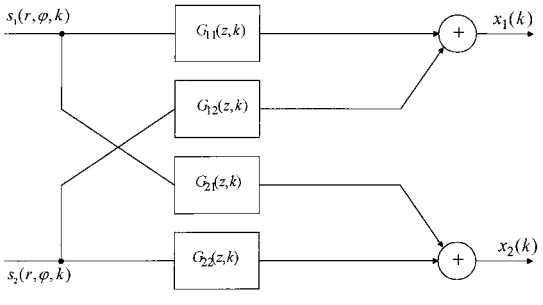

Fig. 6. Modified optical tracker signal model.

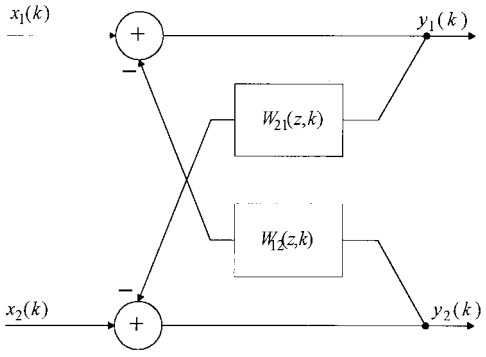

Fig. 7. Feedback separation network.

blind identification problem and the decoupling of the linear combinations is called the BSS problem.[7] In this paper we are considering the BSS problem. Two cases of linear mixture are possible: scalar and convolutive. Since in our application measured signals are a convolutive combination of the source signals [Eqs. (24) and (25)] the convolutive mixing case is treated in this paper. The convolutive mixture is mathematically described as

$$x = G * s, \tag{26}$$

where G is the matrix of impulse responses. For decoupling the convolved signals [see Eqs. (24) and Fig. 6] the feedback-separation network shown in Fig. 7 is used. A feedback-separation network is preferred over a feed-forward network to avoid the whitening effect.[8] Decoupling filters $W_{12}(z)$ and $W_{21}(z)$ must be adjusted so that the transfer function $Q(z) = W(z) \times G(z)$ of the combined system is of the form[9–11]

$$Q(z) = \begin{bmatrix} Q_{11}(z) & 0 \\ 0 & Q_{22}(z) \end{bmatrix} \tag{27}$$

or

$$Q(z) = \begin{bmatrix} 0 & Q_{12}(z) \\ Q_{21}(z) & 0 \end{bmatrix}. \tag{28}$$

In both these cases the source signals are reconstructed to shaping filters $Q_{ij}(z)$. There are three fundamental assumptions on which all BSS algorithms are based: the source signals are statistically independent, the source signals are non-Gaussian, and the mixing matrix in the model of the observed signals is nonsingular. The question of whether these assumptions are fulfilled for the model of the modified optical tracker's output signals [given by Eqs. (24)] are examined briefly at this point. The statistical-independence assumption of source signals $s_1(r, \varphi, t)$ and $s_2(r, \varphi, t)$ is reasonable since they are generated by two different (independent) optical sources. The experimental verification of this assumption is presented in Section 6. Assuming statistical independence, the joint probability density function $f(s)$ of the vector of the source signals is

$$f(s) = \prod_{i=1}^{n} f_i(s_i), \tag{29}$$

where $f_i(s_i)$ is the marginal probability density function of the ith-related component. The second assumption, that the source signals are non-Gaussian, for signals $s_1(r, \varphi, t)$ and $s_2(r, \varphi, t)$ is also fulfilled for the following reasons. Equation (7) shows that the source signals are frequency-modulated signals. These types of signals, like most communication signals, belong to the sub-Gaussian class of signal having negative kurtosis, where kurtosis of signal x is defined as

$$\kappa(x) = \frac{C_4 x}{C_2^{\,2} x}, \tag{30}$$

where C_4x is the fourth-order cumulant and C_2x is the second-order cumulant of signal x. The kurtosis shows how far the signal is from the Gaussian distribution, which has kurtosis equal to zero. This is due to the fact that random processes with Gaussian distributions all have cumulants of the order of 3 or more equal to zero.[12–14] When the two assumptions above hold, all BSS algorithms recover the source signals by minimizing or maximizing certain criteria that indirectly factorize the joint probability density function of the recovered signals. Since the source signals are independent by assumptions, the factorization discussed actually reconstructs the source signals. A consequence of such a separation criteria is that the separated signals in principle represent a scaled and permuted version of the source signals.[7,9,10] The third assumption is the nonsingularity of the mixing matrix when the convolutive model [Eqs. (24)] is transformed into the frequency domain. This transformed model can be written as

$$X(\omega) = G(\omega) \times S(\omega), \tag{31}$$

where $X(\omega)$ and $S(\omega)$ are vectors whose components are discrete Fourier transforms (DFT's) of the observed and the source signals, respectively, while $G(\omega)$ is a matrix whose components are DFT's of the related impulse responses given by Eqs. (25). The nonsingularity requirement of the mixing matrix over some frequency region of interest is formally expressed as

$$\det G(\omega) \neq 0, \qquad \forall \omega \in [\omega_1, \omega_2], \tag{32}$$

where ω_1 and ω_2 are the frequencies determined by the design of the selective amplifiers. The satisfaction of condition (32) is important since it ensures that we benefit from using two sensors. Otherwise both observed signals would deliver the same information and one of them would be redundant. Assuming that the optical flux $\Phi(\lambda, t)$ is piecewise stationary, at least over the time interval determined

by the length of the DFT, the DFT's of the impulse responses [Eqs. (25)] can be written as

$$G_{ij}(\omega) = G_i(\omega) \times k_{ij}, \qquad i, j \in \{1, 2\}, \tag{33}$$

where $G_i(\omega)$ is the DFT of the related selective amplifier impulse responses $g_i(t)$, while k_{ij} can be easily identified from Eqs. (25). Inequality (32) can be rewritten as

$$G_1(\omega)G_2(\omega)[k_{11}k_{22} - k_{21}k_{12}] \neq 0, \quad \forall \omega \in [\omega_1, \omega_2] \tag{34}$$

and is transformed into

$$k_{11}k_{22} - k_{21}k_{12} \neq 0, \tag{35}$$

since in inequality (34) $G_1(\omega)$ and $G_2(\omega)$ represent those frequency responses of the selective amplifiers that are different from zero. Assuming that for the detector spectral responsivities in Eqs. (25) $R_1(\lambda) \cong R_2(\lambda) \cong R(\lambda)$ and taking into account that $\rho(\lambda) = 1 - \tau(\lambda)$, inequality (35) can be transformed into

$$\int_\lambda \frac{\tau(\lambda)R(\lambda)\Phi_1(\lambda)}{\lambda}\,d\lambda \int_\lambda \frac{R(\lambda)\Phi_2(\lambda)}{\lambda}\,d\lambda \neq \int_\lambda \frac{\tau(\lambda)R(\lambda)\Phi_2(\lambda)}{\lambda}\,d\lambda \int_\lambda \frac{R(\lambda)\Phi_1(\lambda)}{\lambda}\,d\lambda. \tag{36}$$

Inequality (36) and consequently inequality (32) is fulfilled when

$$\tau(\lambda) \neq \text{const} \tag{37}$$

over the wavelength region of interest. When actual beam-splitting devices are considered, this is usually the case. Hence the role of the beam splitter is twofold. It ensures, first, that both detectors see the optical sources in the same coordinate system and, second, the nonsingularity of the mixing matrix in the frequency domain. The physical-based reasoning presented in this section gives a framework for designing and performing experiments with the modified optical tracker.

4. Blind Source Separation Algorithms

Ideally, the joint probability density function of the vector of the source signals is factorized when all cross-statistics between components of the signal vector are zero. Provided that non-Gaussian real scalar processes $s_1(r, \varphi, k)$ and $s_2(r, \varphi, k)$ have trispectra that are different from zero, that is,

$$S_{S_iS_iS_iS_i}(\omega_1, \omega_2, \omega_3) \neq 0, \qquad \forall \omega_1, \omega_2, \omega_3 i = 1, 2 \tag{38}$$

and cross-trispectra that are equal to zero, i.e.,

$$S_{S_iS_jS_kS_l}(\omega_1, \omega_2, \omega_3) = 0, \qquad \forall \omega_1, \omega_2, \omega_3 \quad \forall i, j, k, l \in \{1, 2\} \text{ except } i = j = k = l, \tag{39}$$

it was shown in Ref. 9 that the transfer function $Q(z)$ of the combined system will be diagonal when the following conditions are fulfilled:

$$S_{y_1y_1y_1y_2}(\omega_1, \omega_2, \omega_3) = 0, \qquad \forall \omega_1, \omega_2, \omega_3,$$
$$S_{y_2y_2y_2y_1}(\omega_1, \omega_2, \omega_3) = 0, \qquad \forall \omega_1, \omega_2, \omega_3. \tag{40}$$

Equations (40) represent the criteria for signal separation in the frequency domain. The equivalent criteria in the time domain are

$$\text{cum}[y_1(k), y_1(k + \tau_1), y_1(k + \tau_2), y_2(k + \tau_3)] = 0, \quad \forall \tau_1, \tau_2, \tau_3,$$
$$\text{cum}[y_2(k), y_2(k + \tau_1), y_2(k + \tau_2), y_1(k + \tau_3)] = 0, \quad \forall \tau_1, \tau_2, \tau_3. \tag{41}$$

The fourth-order cross-cumulants in Eqs. (41) are obtained as the inverse discrete Fourier transform of the related cross-trispectra [Eqs. (40)].[12,13] This is equivalent to saying that the output signals will be separated when their mutual fourth-order statistics is zero.[9,12] Assuming that $W_{12}(z)$ and $W_{21}(z)$ are finite impulse response filters of orders M_{12} and M_{21}, respectively, the system of equations [Eqs. (41)] is transformed into the system of at least $M_{12} + M_{21}$ linear equations in terms of filter coefficients w_{12} and w_{21}. The solution is obtained by using an iterative algorithm that requires per iteration at least ${M_{12}}^2 + {M_{21}}^2 + M_{12} + M_{21}$ fourth-order sample cross-cumulants to be estimated. Owing to the delay introduced by the block-processing approach and the huge computational complexity of this approach, such a solution is unacceptable for the real-time separation of sources. The discrimination in optical sources (Fig. 6) must be a real-time process. Therefore a real-time version of the BSS algorithms is necessary. Such algorithms are given in Refs. 8 and 15–18 and are adaptive by nature. This means that at every time sample the algorithms should deliver instantaneous values of separated signals $y_1(k)$ and $y_2(k)$. The solution given in Ref. 15 is based on the estimate–maximize algorithm, although the signal-to-noise paradigm still dominates in the approach presented there. In Ref. 16 the adaptive separation is performed by minimizing the instantaneous energy of the separator output signals, which actually decorrelates the signals and does not ensure statistical independence in the true sense. In Ref. 17 several approaches are given, the most interesting of which are neural-network separators based on the products of odd nonlinear activation functions and separators that minimize the squares of fourth-order cross-cumulants such as given in Eq. (41). In Refs. 8 and 18 the separation of the convolved signals is achieved by maximizing the entropy of a sigmoid function of the separator output signals. Here we present a class of adaptive blind separation algorithms for convolved sources based on the information-maximization

principle.[8,18] The input–output relations of the feedback network (Fig. 7) are

$$y_1(k) = x_1(k) - \sum_{i=1}^{M_{12}} w_{12}(i) y_2(k-i),$$
$$y_2(k) = x_2(k) - \sum_{i=1}^{M_{21}} w_{21}(i) y_1(k-i). \quad (42)$$

For causality reasons $w_{12}(0)$ and $w_{21}(0)$ must be zero. It is assumed that source signals $s_1(r, \varphi, k)$ and $s_2(r, \varphi, k)$ have a zero mean and are statistically independent in the sense of Eq. (29). It has been shown in Ref. 18 that the maximization of the information transfer through the sigmoid function $z_i = g(y_i)$ also reduces the redundancy between the outputs of the separation network y_i (Fig. 7). This process is also called independent component analysis, which enables the network to solve the blind separation task. Mutual information between the sigmoid outputs and inputs is defined as[18]

$$I(z, y) = H(z) - H(z/y), \quad (43)$$

where $H(z)$ is the entropy of the sigmoid outputs, while $H(z/y)$ is the residual entropy in the output that did not come from the input. Since in the BSS scenario we have no noise (both signals and noise are treated equally), the entropy $H(z/y)$ has its lowest possible value: It diverges to $-\infty$.[18] So the maximization of the mutual information $I(z/y)$ is equivalent to the maximization of the joint entropy $H(z)$ with respect to the separation filter coefficients:

$$\max_{wij} I(z, y) = \max_{wij} H(z). \quad (44)$$

To show why the maximization of $H(z)$ separates signals y_i [i.e., factorizes joint probability density function $f(y)$], the mutual information (i.e., statistical independence between the components z_i) is expressed in a form of Kullback divergence[19]:

$$MI(z) = \delta\left[f(z), \prod_{i=1}^{n} f_i(z_i)\right] = \int_{-\infty}^{\infty} f(z) \log \frac{f(z)}{\prod_{i=1}^{n} f_i(z_i)} \, dz, \quad (45)$$

where $MI(z)$ vanishes if components z_i are statistically independent; it is strictly positive otherwise.[19] Based on Eq. (45) the mutual information $MI(z)$ can be defined in terms of joint and marginal entropy, $H(z)$ and $H(z_i)$, respectively:

$$MI(z) = -H(z) + \sum_{i=1}^{n} H(z_i), \quad (46)$$

where the entropy terms are defined by[18]

$$H(z) = -E[\log f(z)] = -\int_{-\infty}^{\infty} f(z) \log f(z) dz,$$
$$H(z_i) = -E[\log f(z_i)] = -\int_{-\infty}^{\infty} f(z) \log f_i(z_i) dz. \quad (47)$$

It follows from Eq. (46) that

$$H(z) = \sum_{i=1}^{n} H(z_i) - MI(z). \quad (48)$$

It can be seen from Eq. (48) that the maximization of the joint entropy $H(z)$ actually maximizes the marginal entropy $H(z_i)$ and minimizes mutual information $MI(z)$, which, owing to Eq. (45), leads to the factorization of $f(z)$. Since the z_i terms are related to y_i terms with some invertible transformation, as, for example, $z_i = \tanh(y_i)$, the factorization of $f(z)$ will have as a direct consequence the factorization of $f(y)$. When $z = g(Wx)$ has a unique inverse, the multivariate probability density function can be written as[18]

$$f(z) = \frac{f(x)}{|J|}, \quad (49)$$

where $|J|$ is the absolute value of the Jacobian of the transformation. The Jacobian is defined as the determinant of the matrix of partial derivatives:

$$J = \det\begin{bmatrix} \frac{\partial z_1}{\partial x_1} & \cdots & \frac{\partial z_1}{\partial x_n} \\ \cdot & & \cdot \\ \frac{\partial z_n}{\partial x_1} & \cdots & \frac{\partial z_n}{\partial x_n} \end{bmatrix}. \quad (50)$$

Then, using Eqs. (47) and (49), we can write the joint entropy as

$$H(z) = -E[\ln f(z)] = E[\ln|J|] - E[\ln f(x)]. \quad (51)$$

Now the maximization of $H(z)$ with respect to the coefficients of the separation filters w_{ij} is equivalent to the maximization of $\ln|J|$ since in Eq. (51) $\ln f(x)$ does not depend on w_{ij}. Hence

$$\max_{wij} \mathrm{H(z)} = \max_{wij} \ln|J|. \quad (52)$$

For the feedback separation network shown in Fig. 7 and described with the input–output relation [Eqs. (42)] the absolute value of the Jacobian is

$$|J| = \left|\det\left[\frac{\partial z_i}{\partial x_i}\right]_{ij}\right| = \left|\frac{\partial z_1}{\partial y_1}\frac{\partial z_2}{\partial y_2}\right|. \quad (53)$$

The adjustments of the separation-filter coefficients are then

$$\Delta w_{ij}(k, m) = \frac{\partial H(z)}{\partial w_{ij}(k, m)} = \frac{\partial \ln|J|}{\partial w_{ij}(k, m)} = \frac{\partial}{\partial w_{ij}(k, m)} \ln \frac{\partial z_i}{\partial y_i},$$

$$\Delta w_{ij}(k, m) = \left(\frac{\partial z_i}{\partial y_i}\right)^{-1} \frac{\partial}{\partial w_{ij}(k, m)} \left(\frac{\partial z_i}{\partial y_i}\right), \quad (54)$$

where k is the discrete time index and m is the coefficient index of the related separation filter. If z_i is taken to be $\tanh(y_i)$, then $\partial z_i/\partial y_i = 1 - z_i^2$ and Eq. (54) become

$$\Delta w_{ij}(k, m) = 2z_i(k)y_j(k - m) = 2 \tanh[y_i(k)]y_j(k - m). \quad (55)$$

From this the separator learning rule is

$$w_{ij}(k + 1, m) = w_{ij}(k, m) + \mu\Delta w_{ij}(k, m) = w_{ij}(k, m) + 2\mu \tanh(y_i)y_j(k - m), \quad (56)$$

where μ in Eq. (56) is a small positive constant also called the adaptation gain. The learning rule, [Eq. (56)] is convergent in a statistical sense when the following condition is fulfilled[20]:

$$E[\Delta w_{ij}(k, m)] = 0. \quad (57)$$

Since, by assumption the source signals have zero mean, the mean value of the expression $\tanh(y_i)y_j$ is also equal to zero and consequently

$$E[\Delta w_{ij}(k, m)] = 2E[\tanh[y_i(k)]y_j(k - m)] = 0, \quad (58)$$

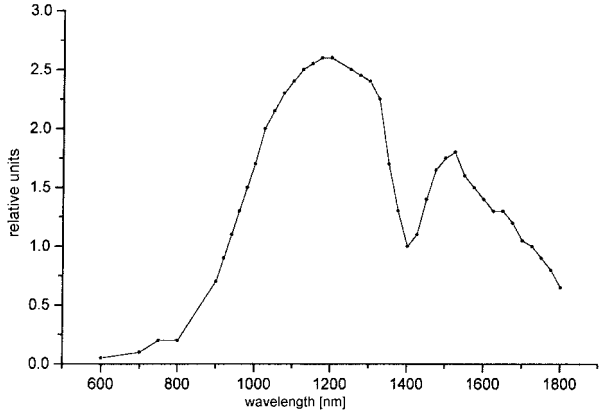

Fig. 8. Relative spectral responsivity of the first optical source.

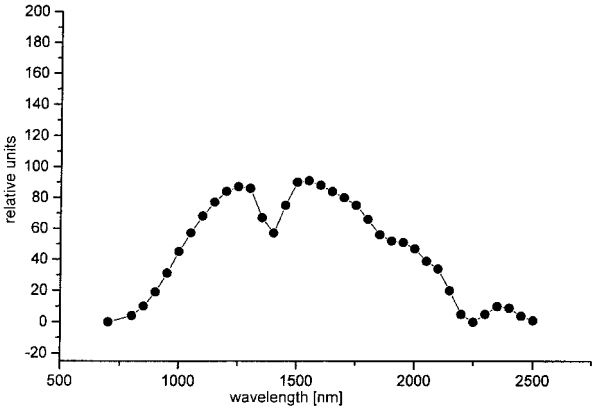

Fig. 9. Relative spectral responsivity of the second optical source.

which proves the convergence of the learning rule [Eq. (56)]. When tanh in Eqs. (55) and (58) is expanded in the Taylor series, Eq. (58) can be written as

$$E[\Delta w_{ij}(k, m)] = E\left[\sum_{l=0}^{\infty} c_{2l+1} y_i^{2l+1}(k)y_j(k - m)\right] = \sum_{l=0}^{\infty} c_{2l+1} E[y_i^{2l+1}(k)y_j(k - m)]. \quad (59)$$

Since, at the equilibrium point $E[\Delta w_{ij}(k, m)] = 0$, the mutual information in Eq. (45) will be minimal, implying that the joint probability density function $f(y)$ will be factorized. This can be written as

$$E[y_i^{2l+1}(k)y_j(k - m)] = E[y_i^{2l+1}(k)]E[y_j(k - m)], \quad (60)$$

which is equal to zero because the y_i terms are zero mean. From Eq. (60) it follows that

$$E[y_i^{2l+1}(k)y_j(k - m)] = 0, \quad (61)$$

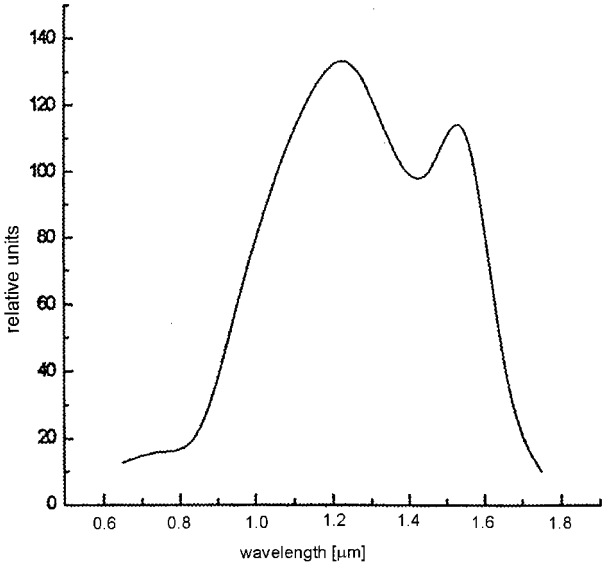

Fig. 10. Ge photodetector spectral responsivity in relative units.

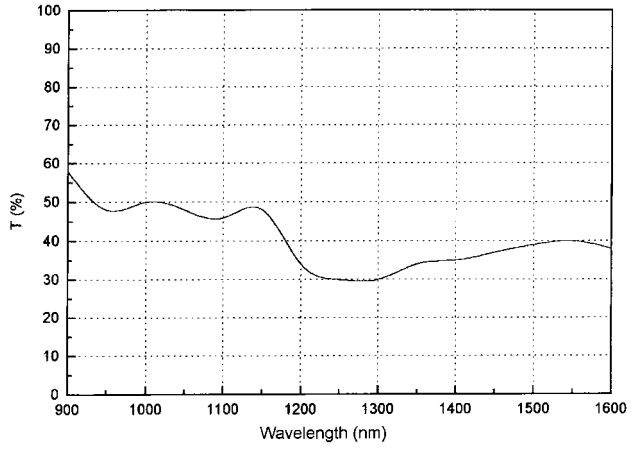

Fig. 11. Beam-splitter transmission coefficient.

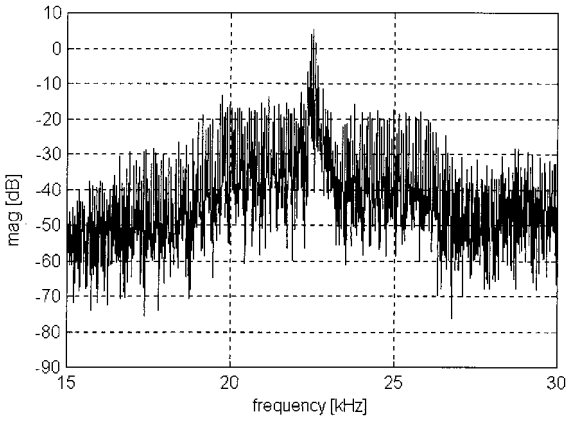

Fig. 13. Power spectrum of the second observed signal.

meaning that the higher-order cross-moments between y_i and y_j are zero, i.e., signals y_i and y_j are statistically independent. The significance of this is that the entropy maximization algorithm ensures that the separator output signals are not only noncorrelated but also statistically independent; i.e., their higher-order cross-correlations are zero.

5. Experimental Results

Two real-world signals were recorded at the output of the modified optical modulator (see Fig. 5) with a sampling frequency of 100 kHz when both optical sources were present in the modified optical tracker field of view. The spectral responsivities expressed in relative units of the first and the second optical source are shown in Figs. 8 and 9, respectively. The spectral responsivity of the Ge photodetector that was used is shown in Fig. 10, while the beam-splitter transmission coefficient is shown in Fig. 11. Note from Fig. 11 that inequality (37), $\tau(\lambda) \neq \text{const}$, has been fulfilled. The power spectra of observed signals $x_1(t)$ and $x_2(t)$ are shown in Figs. 12 and 13, respectively. Information about the position of both optical sources is present in the recorded signals. The first optical source, with a greater radius coordinate, generates a signal with a deviation of ~4 kHz and occupies the spectrum from 18 to 27.5 kHz. The second optical source, with a smaller radius, was located in the center of the modified optical tracker field of view, which corresponds to a carrier frequency of 22.5 kHz, and generates a signal with a deviation of ~20 Hz. The length of the recorded blocks of the observed signals $x_1(t)$ and $x_2(t)$ was 32,768 data samples.

It can be observed from Figs. 12 and 13 that the signal corresponding to the second optical source dominates in the spectrum of both measured signals. When these signals are demodulated by a quadrature FM demodulator, signals with −64 dB of the main harmonic amplitudes are obtained. From Eqs. (7) and (9) the amplitude of that harmonic component is directly proportional to the distance of the optical source projection from the center of the field of view of the modified optical tracker. When the first optical source was present in the tracker's field of view alone, the measured distance was −33.2 dB, while the second optical source was at a distance of −64 dB. This means that by direct demodulation of the observed signals only the second optical source has been distinguished. The results from applying the BSS algorithm based on the learning rule [Eq. (56)] and the separation network shown in Fig. 7 from observed signals $x_1(t)$ and $x_2(t)$ are shown in Figs. 14 and 15.

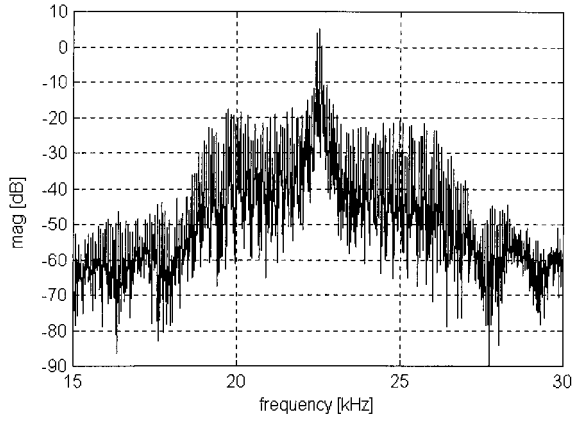

Fig. 12. Power spectrum of the first observed signal.

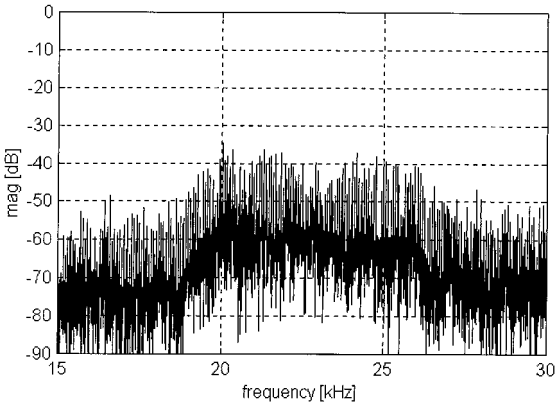

Fig. 14. Power spectrum of the first recovered signal.

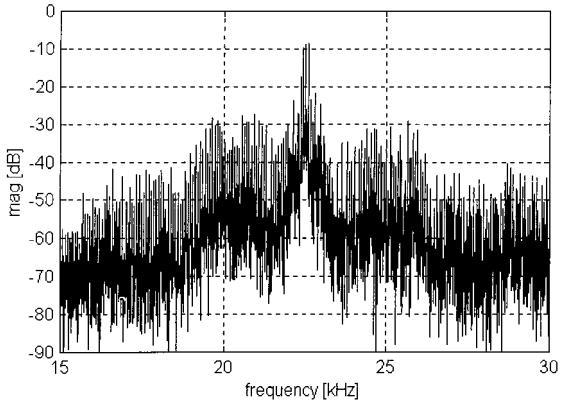

Fig. 15. Power spectrum of the second recovered signal.

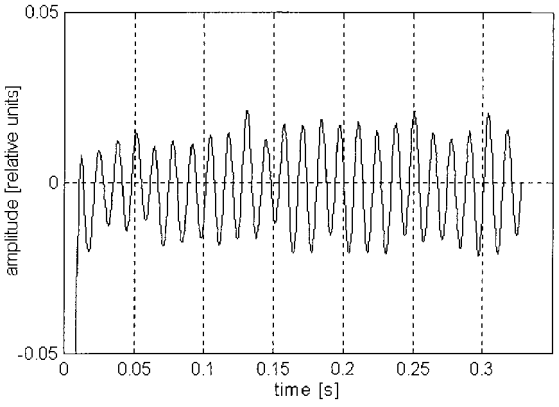

Fig. 17. FM demodulation of the first recovered signal.

As can be seen in Fig. 14 the first optical source is distinguished. The FM demodulation of separated signals $y_1(t)$ and $y_2(t)$ gives signals with the amplitudes of the main harmonic, -35 and -64.4 dB, respectively. So, when entropy-based separation is employed, a 1.8-dB or 19% error is obtained for the first optical source relative to the reference position. Compared with the direct demodulation of the observed signals, the BSS algorithm gives a 29-dB more accurate estimate of the first optical source position. This clearly justifies our approach to distinguishing optical sources by performing blind separation of the responses of the modified optical tracker into independent components. Greater separation accuracy can be expected when BSS is performed in the frequency domain.[21] Here, owing to the orthogonal basis, faster convergence and consequently better separation quality is expected. The time-domain version of the signal obtained by the FM demodulation of the signal generated when only the first optical source was present in the field of view of the tracker is shown in Fig. 16. The signal obtained by the FM demodulation of the separated signal $y_1(t)$ is shown in Fig. 17.

6. Verification of the Statistical-Independence Assumption

The assumption of the statistical independence of source signals $s_1(r, \varphi, t)$ and $s_2(r, \varphi, t)$ is a fundamental assumption on which the BSS theory is based. It was therefore important to verify this hypothesis experimentally by computing the second- and fourth-order cross-statistics between observed signals $x_1(t)$ and $x_2(t)$ and between separated signals $y_1(t)$ and $y_2(t)$. The cross-statistics were computed on the last 4096 points of the related data records. This gives a reliable estimate of the cross-statistics of separated signals y_1 and y_2. The computation of the third-order statistics has no significance since our signals are symmetrically distributed around the dc level, and consequently all odd-order statistics are nearly zero. If separation is successful, $y_1(t)$ and $y_2(t)$ will be the recovered versions of source signals $s_1(r, \varphi, t)$ and $s_2(r, \varphi, t)$. From this it follows that an analysis of the level of statistical independence between separated signals $y_1(t)$ and $y_2(t)$ enables us to draw conclusions regarding the statistical independence of source signals $s_1(r, \varphi, t)$ and $s_2(r, \varphi, t)$. The cross-correlation between observed signals $x_1(t)$ and $x_2(t)$ was computed according to

$$c_{x_1x_2}(\tau) = E[x_1(t)x_2(t+\tau)], \tag{62}$$

where the time lag index τ was running from -500 to 500. Figure 18 shows $c_{x_1x_2}(\tau)$. The cross-correlation of the separated signals $c_{y_1y_2}(\tau)$ was computed similarly and is shown in Fig. 19. The

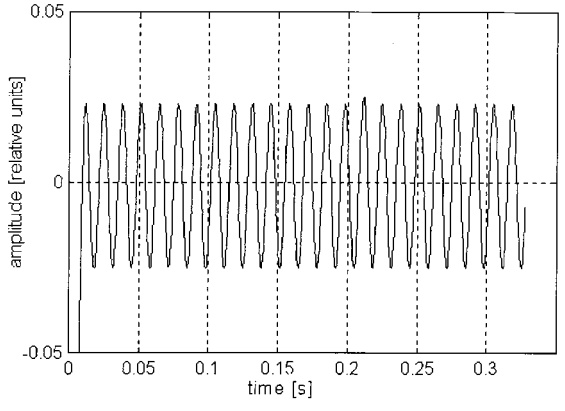

Fig. 16. FM demodulation of the first source signal.

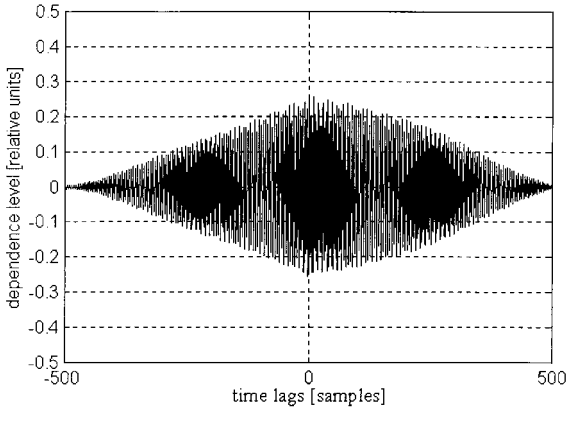

Fig. 18. Cross-correlation between observed signals.

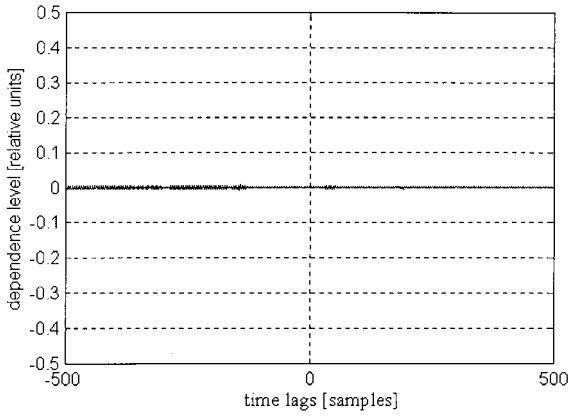

Fig. 19. Cross-correlation between recovered signal.

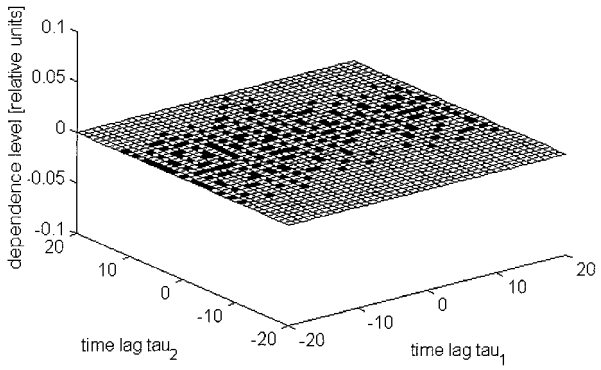

Fig. 21. Fourth-order cross-cumulant C_{22} between recovered signals.

extreme values of the cross-correlation are given by $c_{x_1x_2} = 0.262$ and $c_{y_1y_2} = -0.0067$. The correlation level obtained for $c_{y_1y_2}$ is 39 times smaller than that obtained for $c_{x_1x_2}$. We also computed three fourth-order sample cross-cumulants c_{31}, c_{22}, and c_{13} of signals $x_1(t), x_2(t)$ and $y_1(t), y_2(t)$ to check the fourth-order statistical independence. The fourth-order sample cross-cumulants were computed as[13,14]

$$\begin{aligned} c_{x_ix_jx_kx_l}(\tau_1, \tau_2, \tau_3) &= E[x_i(t)x_j(t+\tau_1)x_k(t+\tau_2)x_l(t+\tau_3)] \\ &\quad - E[x_i(t)x_j(t+\tau_1)]E[x_k(t+\tau_3) \\ &\quad \times x_l(t+\tau_2)] - E[x_i(t)x_k(t+\tau_2)] \\ &\quad \times E[x_l(t+\tau_1)x_j(t+\tau_3)] \\ &\quad - E[x_i(t)x_l(t+\tau_3)]E[x_j(t+\tau_2) \\ &\quad \times x_k(t+\tau_1)], \end{aligned} \tag{63}$$

where τ_3 was set to zero to simplify computation and τ_1 and τ_2 were running from -20 to 20. Based on Eq. (63) $c_{31}(x_1, x_2)$ is computed so that x_i, x_j, and x_k are replaced by x_1 and x_l is replaced by x_2. The values for $c_{22}(x_1, x_2)$, $c_{13}(x_1, x_2)$, $c_{31}(y_1, y_2)$, $c_{13}(y_1, y_2)$, and $c_{22}(y_1, y_2)$ are computed analogously. The extreme values of cross-cumulants c_{13}, c_{22}, and c_{31} of observed signals x_1 and x_2 are -0.0533, -0.112, and -0.1097, respectively. The extreme values of the corresponding cross-cumulants of the separated signals y_1 and y_2 are 8.545×10^{-4}, 3.885×10^{-4}, and 4.669×10^{-5}. Figures 20 and 21 show cross-cumulants $c_{22}(x_1, x_2)$ and $c_{22}(y_1, y_2)$, respectively. Separated signals $y_1(t)$ and $y_2(t)$ have a fourth-order statistical dependence level that is from 62 to 2350 times smaller than observed signals $x_1(t)$ and $x_2(t)$. This confirms the assumption concerning the statistical independence of the source signals. The claim that output signals $y_1(t)$ and $y_2(t)$ will be separated when they are statistically independent is thus also verified experimentally.

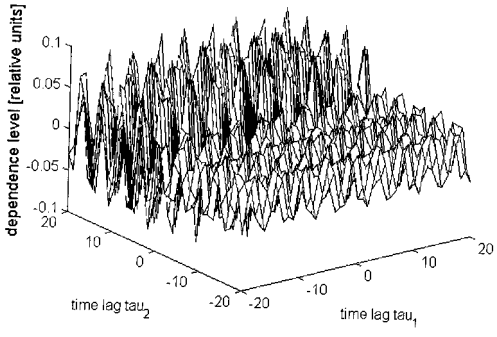

Fig. 20. Fourth-order cross-cumulant C_{22} between observed signals.

7. Conclusion

We have presented a solution in principle for the reduction of errors in optical trackers that see several sources. The design of the optical tracker has been modified by the introduction of one or more beam splitters and the appropriate number of photodetectors and photoamplifiers. By combining optical modulation theory, semiconductor photodetection theory, and linear filtering theory, we have shown that the photoamplifier output signals are convolved combinations of reticle-modulating functions, which carry information about the polar coordinates of the optical sources and the time-varying impulse responses. It has been demonstrated experimentally that by application of BSS algorithms on the output signals of the modified optical tracker it is possible (in principle) to recover unknown non-Gaussian source signals (modulating functions), assuming that the time-varying impulse responses are also unknown. When the source signals are recovered, the determination of the coordinates of each optical source is simply a matter of demodulation of the corresponding recovered source signal. The assumption about the statistical independence of the source signals was also verified experimentally. By overcoming these multisource limitations of the optical trackers, we show that such systems may be of interest for further development.

References

1. R. D. Hudson, Jr., "Optical modulation," in *Infrared System Engineering* (Wiley, New York, 1969), Chap. 6, pp. 235–263.
2. G. F. Aroyan, "The technique of spatial filtering," Proc. Inst. Radio Eng. **47,** 1561–1568 (1959).
3. T. B. Buttweiler, "Optimum modulation characteristics for

amplitude-modulated and frequency-modulated infrared systems," J. Opt. Soc. Am. **51,** 1011–1015 (1961).
4. A. F. Nicholson, "Error signals and discrimination in optical trackers that see several sources," Proc. IEEE **53,** 56–71 (1965).
5. H. Taub and D. L. Schilling, "Frequency-modulation systems," in *Principles of Communication Systems* (McGraw-Hill, New York, 1987), Chap. 4, pp. 142–182.
6. J. Singh, "Optoelectronic detectors," in *Semiconductor Optoelectronics—Physics and Technology* (McGraw-Hill, New York, 1995), Chap. 7, pp. 336–398.
7. X. R. Cao and R. W. Liu, "General approach to blind source separation," IEEE Trans. Signal Process. **44,** 562–571 (1996).
8. K. Torkkola, "Blind separation of convolved sources based on information maximization," in *IEEE Workshop on Neural Networks for Signal Processing, Kyoto, Japan*, 4–6 September, 1996 (Institute of Electrical and Electronics Engineers, New York, 1996).
9. D. Yellin and E. Weinstein, "Criteria for multichannel signal separation," IEEE Trans. Signal Process. **42,** 2158–2168 (1994).
10. D. Yellin and E. Weinstein, "Multichannel signal separation: methods and analysis," IEEE Trans. Signal Process. **44,** 106–118 (1996).
11. J. Wang and H. Zhenya, "Blind identification and separation of convolutively mixed independent sources," IEEE Trans. Aerospace Electron. Syst. **33,** 997–1002 (1997).
12. D. R. Brillinger, "Foundations," in *Time Series Data Analysis and Theory* (McGraw-Hill, New York, 1981), Chap. 2, pp. 16–44.
13. J. M. Mendel, "Tutorial on higher-order statistics (spectra) in signal processing and system theory: theoretical results and some applications," Proc. IEEE **79,** 278–305 (1991).
14. P. McCullagh, "Elementary theory of cumulants," in *Tensor Methods in Statistics* (Chapman & Hall, London, 1987, 1995), Chap. 2, pp. 24–46.
15. E. Weinstein, A. V. Oppenheim, M. Feder, and J. R. Buck, "Iterative and sequential algorithms for multisensor signal enhancement," IEEE Trans. Signal Process. **42,** 846–859 (1994).
16. S. Van Gerven and D. Van Compernolle, "Signal separation by symmetric adaptive decorrelation: stability, convergence, and uniqueness," IEEE Trans. Signal Process. **43,** 1602–1612 (1995).
17. H. L. Nguyen Thi, C. Jutten, and J. Caelen, "Speech enhancement: analysis and comparison of methods on various real situations," in *Signal Processing VI: Theories and Applications*, J. Vandewalle, R. Boite, and A. Oosterlick, eds. (Elsevier, New York, 1992), pp. 303–306.
18. A. J. Bell and T. J. Sejnowski, "An information-maximization approach to blind separation and blind deconvolution," Neural Comput. **7,** 1129–1159 (1995).
19. P. Common, "Independent component analysis, a new concept?" Signal Process. **36,** 287–314 (1994).
20. E. Sorouchyari, "Blind separation of sources, Part III: Stability analysis," Signal Process. **24,** 21–29 (1991).
21. P. J. Smaragdis, "Blind separation of convolved mixtures in the frequency domain," in *International Workshop on Independency and Artificial Neural Networks, Tenerife, Spain*, 9–10 February, 1998 (University of Laguna, Tenerife, Spain, 1998).